DOI: http://doi.org/10.4038/sljp.v23i1.8114

INSTITUTE OF PHYSICS – SRI LANKA

Research Article

Preliminary optimization of low-cost quasi solid-state dye sensitized solar cells with multilayer photoanodes, and graphite-based counter electrodes

H. M. N. Wickramasinghe*, K. Wijayaratne and T. M. W. J. Bandara

Department of Physics and Postgraduate Institute of Science, University of Peradeniya, Peradeniya, Sri Lanka.

Abstract

Investigation and development of platinum free counter-electrodes are highly important in preparing low-cost Dye-Sensitized Solar Cells (DSSCs). In this study, low-cost graphite and TiO_2 composite counter-electrodes are investigated along with photo-electrodes containing dye-photosensitized (N719) TiO_2 multilayers (five, six, and seven layers).

The highest DSSC efficiency is observed for the cells assembled using the counter-electrode that contains 80% of graphite and 20% TiO_2, for all the multilayer photo-electrode series investigated. When comparing different series of multilayer photo-electrodes assembled with this optimized counter-electrode composition, the DSSC efficiency for the six-layer series is greater than the five and seven-layer electrodes.

This best composition of electrodes optimizes the efficiency by fine-tuning between the charge carrier transport properties and catalytic activity of the electrode. The graphite content plays a significant role due to its catalycity. In 3 hours under irradiation, open-circuit voltage got reduced by 8.0%, while the current density and efficiency got improved by 43.2% and 7.0%, respectively, as observed for the cells with the optimum electrode combination. It can be determined that Graphite/TiO_2 80%/20% counter-electrodes with six-layer photoelectrodes optimize the performance of platinum free low-cost DSSCs.

Keywords: Dye-sensitized Solar Cell, Low-Cost Counter-electrode, and Graphite/TiO_2 Composite.

* Corresponding author: narmadawick@gmail.com

1. INTRODUCTION

Most of the dye-sensitized solar cells (DSSCs) currently being developed use platinum as the counter-electrode material, which is an expensive material, despite its superior electro-catalytic activity[1,2]. When searching for a cost-effective alternative to platinum, critical properties are conductivity, durability against iodine corrosion, high catalytic activity, and cell stability. Graphite is an emerging replacement for platinum for DSSC counter-electrodes[3]. Most of the testified studies on carbonaceous counter-electrodes have been developed with liquid electrolytes, with adverse effects on cell stability and longevity. The primary issue with carbonaceous counter-electrodes is the insufficient adhesion to the substrate. Overcoming this, leading to good film formation, is crucial in improving the efficiency of the DSSCs while reducing the cost[4]. This study explores an effective solution for these issues by developing composite counter-electrodes consisting of graphite and TiO_2 nanoparticles, along with optimizing the number of layers on photo-electrodes[5]. First, several series of counter-electrodes were developed by altering the chemical composition. Then their performances were investigated by assembling cells with three different multi-layered TiO_2 working electrodes sensitized with N719 dye[6].

To reduce the well-known instability issues in liquid electrolytes, we used an improved gel polymer electrolyte in the presented study[7]. A previously optimized gel polymer electrolyte comprised of 4-tert-butyl pyridine (4TBP), ethylene carbonate (EC), 1-butyl-3 methylimidazolium iodide (BMII), propylene carbonate (PC), lithium iodide (LiI), tetrahexylammonium iodide (Hex_4NI), and polyethylene oxide (PEO) was utilized in this work[2,5].

2. METHODOLOGY

A series of counter-electrodes were developed by mixing graphite and TiO_2. Table 1 shows relevant weights of TiO_2 nanoparticles (21 nm) and commercial graphite powder. A slurry was obtained by adding 0.1M HNO_3 (2 ml) and was then coated on fluorine-doped tin oxide (FTO) substrate. The films were annealed at 450 °C (30 minutes) to complete the counter-electrode preparation.

Table 1. Weight proportions of TiO_2 and graphite in deferent counter-electrodes.

Electrode	Graphite /wt.%	TiO_2 % /wt.%
A	100	0
B	90	10
C	80	20
D	70	30
E	60	40
F	50	50

To investigate the layering effect of photo-electrodes, 5, 6, and 7 layers of TiO_2 were coated on FTO substrates. In the preparation, a slurry of TiO_2 nanoparticles (∽13 nm) prepared by mixing 0.5 g of TiO_2 with 2 ml of (0.1M) HNO_3 was spin-coated at 2300 rpm for around 2 minutes. After air-drying for ∽5 h, the prepared electrodes were sintered at 450 °C for 30 minutes[8]. The 2nd layer was prepared using the same process, by spin coating at 1000 rpm for about 2 minutes. For the 3rd layer, another TiO_2 dispersion was prepared by grinding 0.5 g of larger TiO_2 nanoparticles (∽21 nm) with 2 ml of 0.1M HNO_3[9]. The resultant dispersion was then spin-coated (1000 rpm, 2 minutes) followed by sintering at 450 °C. Then the subsequent 4th, 5th, 6th, and 7th layers were coated by repeating the same method [8]. The prepared electrodes were immersed in a 0.5 mM N719 dye/ethanol solution for 48 h [9]. Finally, a series of DSSCs were assembled by sandwiching the pre-optimized gel electrolyte between the electrodes[10].

Current-voltage (*I-V*) characteristics of Graphite/TiO_2 electrodes were measured to find sheet resistance values. For this purpose, Graphite/TiO_2 films were deposited on a glass substrate. The X-Ray Diffraction (XRD) and Scanning Electron Microscopic (SEM) images were used for the structural and morphological characterization of Graphite/TiO_2 composite counter-electrodes. In order to study the solar cell performance, the DSSCs were irradiated by the solar simulator (AM1.5, 1000 W m^{-2}) and *I-V* parameters were measured.

3. RESULTS AND DISCUSSION

3.1. Structure and morphology of the counter-electrodes

Scanning Electron Microscopic images (SEM) of the six counter-electrodes are given in Figure 1. According to Figure 1, the film with 100% graphite (Fig. 1-A) yields high reflectance at grain boundaries, and the density of such boundaries is higher. In addition, it

was observed that the film formation is poor for this composition. When the TiO_2 content increases, the density of these reflective domains declines, which may be due to the materialization of expanded graphite during the vigorous stirring.

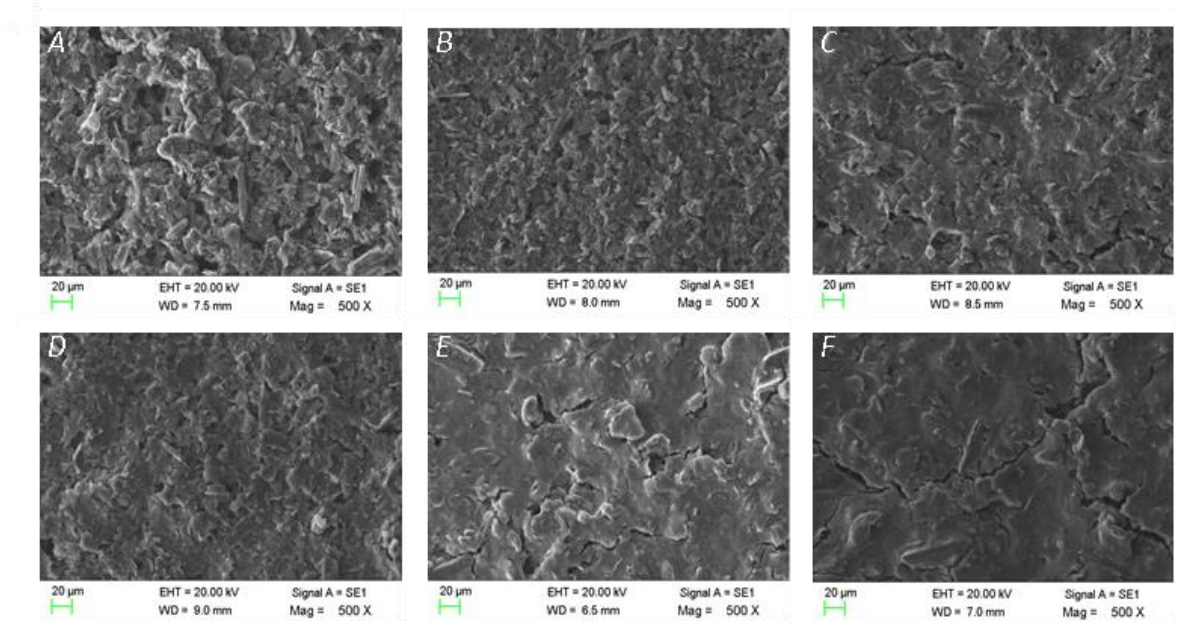

Figure 1: SEM images of counter-electrodes made of Graphite/TiO_2 composite at 500 magnification with varying graphite composition (A) 100% (B) 90% (C) 80% (D) 70% (E) 60% (F) 50% by weight.

The sheet resistance measurements obtained for the Graphite/TiO_2 thin films coated on soda-lime glass plates are given in Table 2. The calculated resistivity and conductivity values are also provided. The average thickness of Graphite/TiO_2 layers was about 0.14 mm. The electrodes with 80% and 70% graphite content demonstrated relatively low sheet resistance and high conductivity. Poor film formation and weak adhesivity to the substrate of 100% graphite samples would have resulted in a slightly lower conductivity. 50% graphite samples demonstrated the lowest conductivity out of all measured samples, which can be attributed to the presence of an excessive amount of low-conducting TiO_2. The highest conductivity value of 1.30 S cm^{-1} was exhibited by the electrode that contained 70 wt.% graphite and 30 wt.% TiO_2.

X-ray diffraction (XRD) was used to investigate the effects of the Graphite/TiO_2 composition on the film structure (Figure 2). XRD spectra in Figure 2 indicate the absence of chemical interactions between TiO_2 and Carbon. However, it can be inferred that the effective exfoliation of graphite into expanded graphite or multilayer graphene has happened since a relative peak broadening is observed with the increasing centration of TiO_2.

Table 2. Resistivity and conductivity values obtained from sheet resistance values of the Graphite/TiO_2 electrodes with various compositions.

Sample	Graphite /wt. %	Sheet Resistance /∧ cm^{-2}	Resistivity /∧ cm	Conductivity /S cm^{-1}
A	100	123.53 ± 0.01	1.73 ± 0.12	0.58 ± 0.04
B	90	89.35 ± 0.01	1.25 ± 0.09	0.80 ± 0.08
C	80	57.56 ± 0.01	0.81 ± 0.06	1.24 ± 0.18
D	70	54.84 ± 0.01	0.77 ± 0.06	1.30 ± 0.20
F	60	63.90 ± 0.01	0.89 ± 0.06	1.12 ± 0.15
F	50	1553.83 ± 0.01	21.75 ± 1.55	0.05 ± 0.00

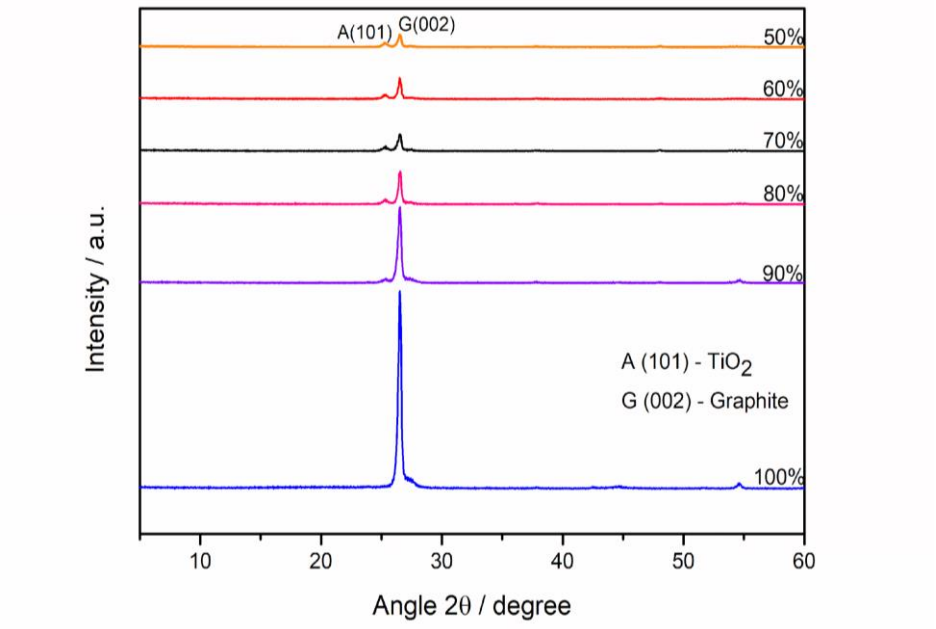

Figure 2: XRD patterns of Graphite/TiO_2 electrode series with different compositions

3.2. Structure and morphology of multilayer photo-anode

XRD spectra of photoelectrodes were used to examine the crystal structure of the photoelectrodes. There were no significant changes among the crystalline structures of 5, 6, and 7 layered TiO_2 films, and thus, the XRD spectrum of six-layered TiO_2 electrodes is shown in Figure 3. All the samples exhibited peaks corresponding to Anatase (101, 004, 200) and Rutile (110, 211, 220, 002, 310) crystal planes.

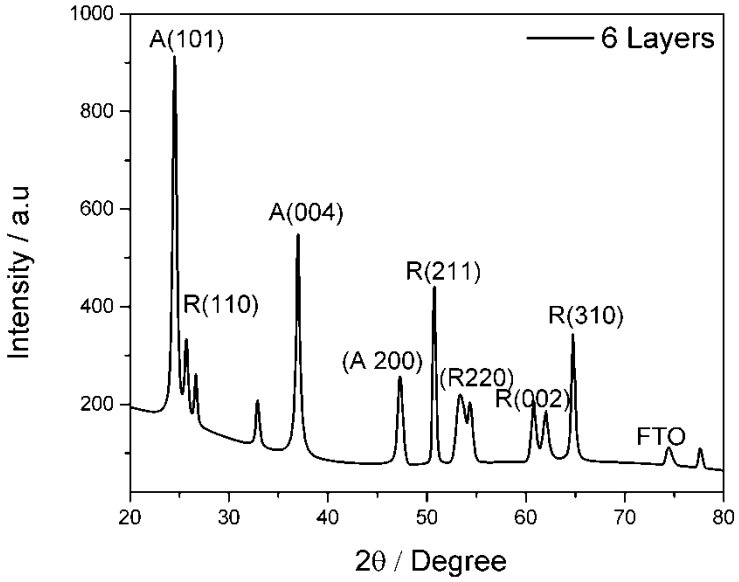

Figure 3: XRD spectra of six-layer photoelectrode

Table 3: XRD analysis data for six-layer TiO_2 film

$2\boldsymbol{\theta}$ / Degree	Peak Height / a.u.	Peak Intensity (a.u.)	FWHM / Degree	*d* Spacing / Å
24.50	746.31	459.39	0.50	3.63
25.70	174.87	135.99	0.46	3.46
37.00	488.38	259.41	0.42	2.43
50.75	359.29	151.75	0.39	1.80
64.75	267.71	159.48	0.45	1.44

3.3 Optimization of counter-electrode composition

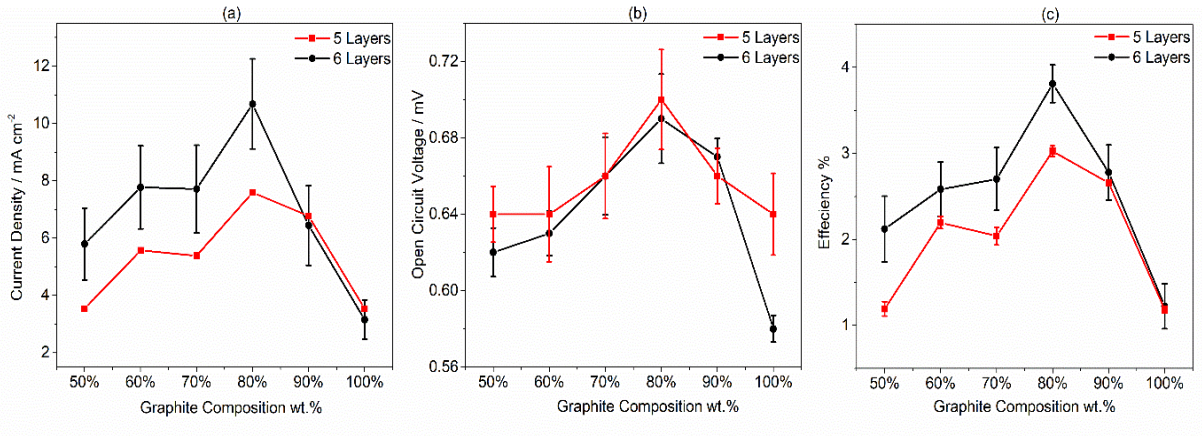

Figure 4. (a) The current density (b) open-circuit voltage and (c) efficiency; versus graphite composition in the counter-electrode for the two series of DSSCs

In order to find the optimum counter-electrode composition, several DSSCs were prepared by changing the composition of the counter-electrode. Two such series were investigated using five and six-layered photo-anodes. Figure 4 shows circuit current density (J_{SC}), open-circuit voltage (V_{OC}), and energy conversion efficiency as a function of graphite composition

in the counter-electrode for both the series of DSSCs. It can be concluded that 80% graphite and 20% TiO_2 containing counter-electrode is optimum for DSSCs. This can be due to the combined effect of the high conductivity of the counter-electrode and the high electro-catalytic activity due to graphite.

3.4 Optimization of the photo-anode

The composition-optimized counter-electrode was selected to study the effect of the number of TiO_2 layers in the photo-anode. The variations of the J_{SC} against the cell potential is shown in Figure 5 (a) in Figures 6 (b), respectively for 5, 6, and 7 -layer series of photoanodes prepared using the above-mentioned optimized counter-electrode.

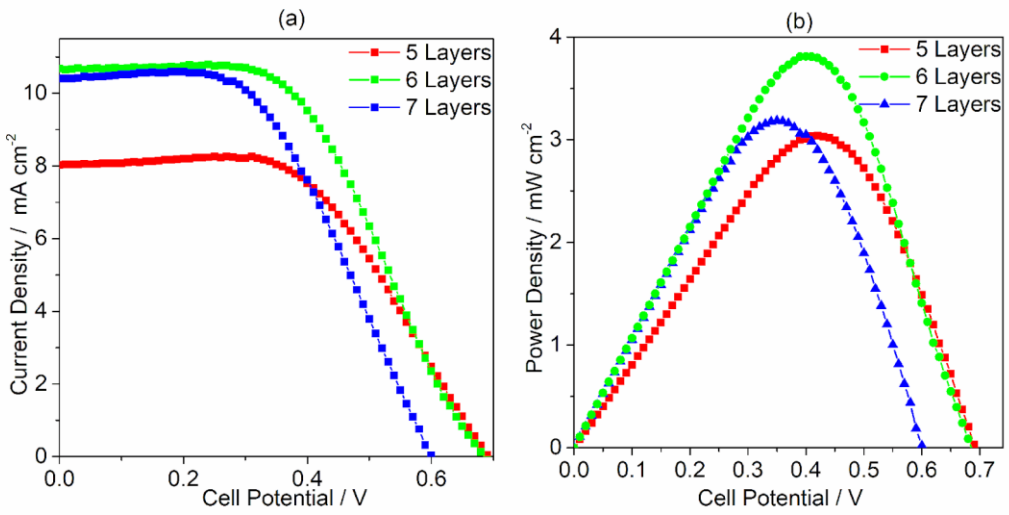

Figure 5. (a) The power density and (b) Current density vs. cell potential for optimized counter electrode (80% graphite)

The highest efficiency (3.81%) was observed for the DSSC with the counter-electrode that contained 80 wt.% graphite with 6-layer photo-anode. This configuration surpassed the efficiency of the counter-electrode with the maximum conductivity (2.7%, at 70 wt.% graphite) due to the greater catalycity of its graphite-rich (80%) composition. J_{SC} and V_{OC} were 10.68 ± 0.345 mA cm^{-2} and 0.69 ± 0.01 mV respectively for DSSCs with six-layer photoanode and optimized counter-electrode. For five-layer photoanode series, the highest efficiency (3.03%) was still exhibited by the DSSC with Graphite/TiO_2 electrode that confined 80 wt.% graphite. The optimized J_{SC} and V_{OC} were 7.59 ± 0.345 mA cm^{-2} and 0.70 ± 0.01 mV.

3.5 Stability

In addition, the short-term stability of the optimized cell was monitored continuously by obtaining *J-V* curves for about 3 hours. Despite the cells being unsealed, they were significantly stable within the three-hour period due to the use of the improved gel polymer electrolyte. The efficiency gradually increased throughout the illumination period and is evident by the dramatic increase in photocurrent density and the drop in V_{OC}. This behavior can mainly be attributed to the ionic conductivity improvement of the electrolyte upon increasing temperature under continuous irradiation. The same phenomena resulted in the drop of the V_{OC} upon increased recombination of excited electrons in the photoelectrode with tri-iodide in the electrolyte. At the end of three hours, V_{OC} was reduced by 8.0%, while J_{SC} improved by 43.2%, leading to an efficiency increase of about 7.0%. It is planned to measure the long-term stability by sealing these quasi-solid state solar cells.

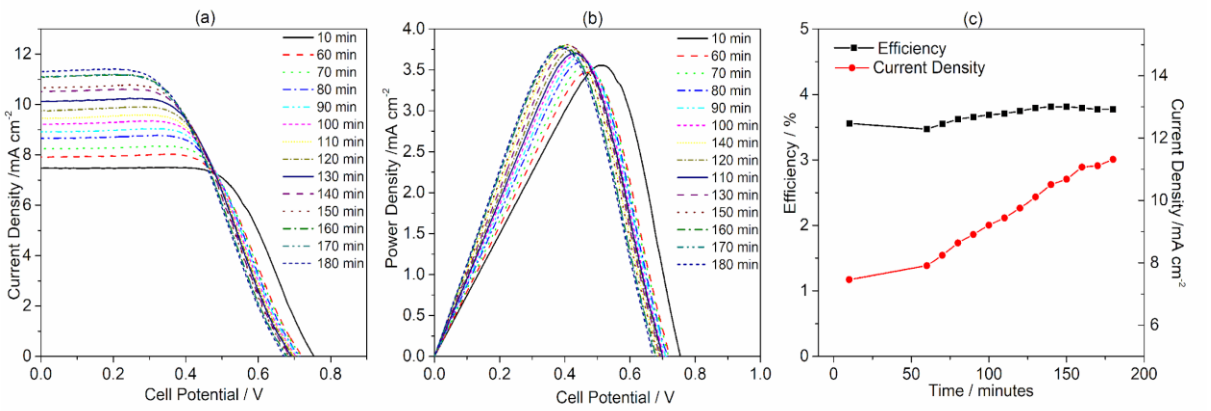

Figure 6. The time dependence of the (a) current density and (b) power density versus cell potential (c) Time verses efficiency and current density variation of DSCs with 80% graphite counter-electrode

4. CONCLUSION

The cost-effective counter-electrodes were developed using TiO_2 nanoparticles and commercial graphite to substitute costly platinum counter-electrodes in dye-sensitized solar cells. The highest DSSC efficiency was observed for the counter-electrode composed of 80% graphite and 20% TiO_2 by optimizing the trade-offs between charge carrier transport and the electro-catalycity. This optimum composition ratio was confirmed by using two series of DSSCs having 5 and 6 TiO_2 layers in the photo-anode.

Further, it was confirmed that the 6 layer TiO_2 photoanode gives the highest DSSC performance by investigating 7 layer photo-anodes alongside 5 and 6 layer versions. The DSSCs gave the highest efficiency (3.81%) with counter-electrodes containing 80 wt.%

graphite with photo-anodes having 6 TiO_2 layers. The optimized cells exhibited very good short-term stability within three hours of continuous illimitation, and there were no traces of efficiency drop. It can be concluded that 6-layer photo-anodes assembled with 80/20 wt.% Graphite/TiO_2 counter-electrode is the optimum electrode combination to prepare cost-effective DSSCs.

Acknowledgment

The authors gratefully acknowledge the support received via the Postgraduate Institute of Science (PGIS), University of Peradeniya research grant (No. PGIS/2020/05).

REFERENCES

[1] Iqbal, M. Z. and Khan, S. (2018) "Progress in the performance of dye sensitized solar cells by incorporating cost effective counter electrodes," *Sol. Energy*, vol. 160, pp. 130–152.

[2] Nishshanke, M., Arof, A. K., and Bandara, T., (2020) "Review on mixed cation effect in gel polymer electrolytes for quasi solid-state dye-sensitized solar cells," *Ionics (Kiel).*, vol. 26.

[3] Salvatierra, R. V., Domingues, S. H., Oliveira, M. M. and Zarbin, A. J. G., (2013) "Tri-layer graphene films produced by mechanochemical exfoliation of graphite," *Carbon N. Y.*, vol. 57, pp. 410–415.

[4] Denaro, T., *et al.*, (2009) "Investigation of low cost carbonaceous materials for application as counter electrode in dye-sensitized solar cells," *J. Appl. Electrochem.*, vol. 39, no. 11, pp. 2173–2179.

[5] Yousif, Q. A., Mahdi, K. M., and Alshamsi, H. A., (2021) "Enhanced photovoltaic performance of dye-sensitized solar cell based on ZnO nanoparticles and ZnO/graphene nanocomposites," *J. Chinese Chem. Soc.*, vol. 68, no. 9, pp. 1637–1643.

[6] Bandara,T. M. W. J., *et al.*,(2015) "Efficiency of 10 % for quasi-solid state dye-sensitized solar cells under low light irradiance," *J. Appl. Electrochem.*, vol. 45, no. 4, pp. 289–298.

[7] Bandara, T. M. W. J., Dissanayake, M. A. K. L., Jayasundara, W. J. M. J. S. R., Albinsson, I., and Mellander, B. E., (2012) "Efficiency enhancement in dye sensitized solar cells using gel polymer electrolytes based on a tetrahexylammonium iodide and MgI 2 binary iodide system," *Phys. Chem. Chem. Phys.*, vol. 14, no. 24, pp. 8620–8627.

[8] Nishshanke,G. B. M. M. M., Thilakarathna B. D. K. K., Albinsson I., Mellander B. E., and Bandara, T. M. W. J.,(2021) "Multi-layers of TiO2 nanoparticles in the photoelectrode and

binary iodides in the gel polymer electrolyte based on poly(ethylene oxide) to improve quasi solid-state dye-sensitized solar cells," *J. Solid State Electrochem.*, vol. 25, no. 2, pp. 707–720.

[9] Bandara, T. M. W. J., Wickramasinghe, H. M. N., Wijayaratne, K., DeSilva, L. A., and Perera, A. A. I., (2020) "Quasi-solid-state dye-sensitized solar cells utilizing TiO2/graphite composite counter electrode and TiO2/N719 sensitizer photoelectrode for low-cost power generation," *J. Mater. Sci. Mater. Electron.*, vol. 32, no. 22, pp. 26758–26769.

[10] Il Kim, M., Cho, J. H., Bai, B. C., and Im, J. S., (2020) "The control of volume expansion and porosity in carbon block by carbon black (CB) addition for increasing thermal conductivity," *Appl. Sci.*, vol. 10, no. 17.